Progress In Electromagnetics Research C, Vol. 68, 31–44, 2016

Design of Single-Band to Hexa-Band Bandstop Filters

Ashwani Kumar[1, *], Anand K. Verma[2, 3], Qingfeng Zhang[4], Parmod Kumar[5], Praduman P. Singh[1], Rajendar P. Rishishwar[1], Abhishek Singh[1], Ankita Bansal[1], and Ritu[1]

Abstract—This paper presents a systematic design process to design Bandstop Filters from Single-Band (SB-BSF) to Hexa-Band (HB-BSF). The presented BSFs are useful to suppressing the unwanted signal frequencies from 1.98 GHz to 7.75 GHz. Single-Band BSF suppress the frequency 1.98 GHz; Dual-Band BSF suppress 2 GHz and 3.4 GHz (WiMax Band); Triple-Band BSF suppress 2.0 GHz, 3.4 GHz, and 4.75 GHz; Quad-Band BSF suppress 2.0 GHz, 3.4 GHz, 4.75 GHz, and 6.4 GHz; Penta-Band suppress 2.0 GHz, 3.4 GHz, 4.0 GHz, 4.85 GHz, and 6.75 GHz; however Hexa-Band suppress 2.0 GHz, 3.4 GHz, 4.2 GHz, 4.75 GHz, 6.5 GHz, and 7.75 GHz. The attenuation level for the suppressed frequencies varies from 19 dB to 62 dB, and the quality factor varies from 17 to 384.5. The simulated and measured results are presented to validate the design process. Such compact BSFs could be useful in modern communication systems to stop the potential interference of the unwanted signal frequencies in WLAN and UWB bands.

1. INTRODUCTION

Nowadays multifunctional wireless integrated communication systems become more and more important and have been used for miniaturization of the communication equipment. In recent years, plenty of works have been done on integrated and multifunctional wireless communication systems. Multi-Band Bandstop filters play an important role and are tremendously preferred, which can be simultaneously used for stopping different signal frequencies. Some effective methods have been proposed to develop Single-Band [1] Dual-Band [2–6] and Triple-Band Bandstop filters [7–14]. However, the design of Triple-Band Bandstop filters (TB-BSFs) and controlling the stopband frequencies within the specified band are difficult. Hence, relatively few works have been done on TB-BSFs [7–14]. Some TB-BSFs are designed by using series LC resonators and admittance inverters [7], T-shaped defected microstrip structure [8], cross-coupling stubs [9], square patch resonator [10], defected microstrip structure (DMS) and E-shaped defected ground structure (DGS) with open-loop resonators coupled to the microstrip line [11], U-shaped DGS [12], Hilbert-Fork resonator [13] and by using meander line stepped impedance resonator [14]. These TB-BSFs are very useful for suppressing the three spurious signals. The Quad-Band Bandstop filters (QB-BSFs) are very difficult to design; recently just three popular QB-BSFs are designed using defected microstrip structure (DMS) and E-shaped defected ground structure (DGS) with open-loop resonators coupled to the microstrip line [15], using two shunt-connected tri-section stepped-impedance resonators (TSSIRs) [16] and open-circuited stubs [17]. However, to the best of

Received 30 May 2016, Accepted 16 August 2016, Scheduled 4 October 2016

* Corresponding author: Ashwani Kumar (ashwanikumar7@yahoo.com).

[1] Department of Electronics, Sri Aurobindo College, University of Delhi, Malviya Nagar, New Delhi-110017, India. [2] Microwave Research Laboratory, Department of Electronic Science, University of Delhi South Campus, New Delhi-110021, India. [3] Department of Electronics, Macquarie University, NSW, Sydney, Australia. [4] Department of Electrical and Electronics Engineering, South University of Science and Technology of China (SUSTC), 518055, China. [5] Department of Chemistry, Sri Aurobindo College, University of Delhi, Malviya Nagar, New Delhi-110017, India.

our knowledge, no Bandstop filters with Penta-Band and Hexa-Band characteristics are designed and proposed. It is an interesting area for researchers to design a Multi-Band Bandstop filters.

In this paper, six Bandstop filters are presented. The proposed Bandstop filters are useful for the Single-Band to Hexa-Band applications. Single-Band BSF (SB-BSF) is designed by using two folded U-slots, Dual-Band BSF (DB-BSF) is designed using three folded U-slots, TB-BSF is designed using three different sizes folded U-slots, QB-BSF is designed using three different sizes folded U-slots in microstrip line and two folded U-slots in the ground plane. Penta-Band and Hexa-Band BSFs are designed using three different sizes folded U-slots in microstrip line and ground plane with one coupled S-type resonator. The proposed designed methodology is simple and systematic. Proposed Multi-Band Bandstop filters are useful for IEEE 802.11a WLAN band in the ranges (5.15–5.25 GHz, 5.25–5.35 GHz, 5.47–5.725 GHz, 5.725–5.825 GHz), as well as IEEE 802.11b band in the range 2.412–5.484 GHz, WiMax (3.4 GHz), GSM (1.8 GHz), and S-band (2.0 and 2.2 GHz) for Mobile Satellite Service (MSS) networks in connection with Ancillary Terrestrial Components (ATC) [19]. Finally, some of the Multi-Band Bandstop filters are fabricated, and their performances are measured to verify the concept.

2. DESIGN OF SINGLE-BAND TO TRIPLE-BAND BANDSTOP FILTERS

This section presents the design of the SB-BSFs to the TB-BSFs by using the microstrip line with embedded folded U-slots. These three filters are useful to stop the unwanted signal frequency from 1.98 GHz to 4.75 GHz in the WLAN and UWB band. An FR-4 substrate with relative permittivity $\varepsilon_r = 4.4$, $h = 1.6$ mm has been used to design these Bandstop filters, and simulation has been carried out on 3D EM software HFSS v11 [20].

2.1. Single-Band Bandstop Filter (SB-BSF)

This section presents the design of SB-BSF. Initially, to design the SB-BSF, we have considered single folded U-slot in microstrip line. Single folded U-slot provides two resonance frequencies at 2.0 GHz and 6.2 GHz with 8 dB and 4 dB attenuation levels, respectively. Further adding another same size folded U-slot in the microstrip line gives Single-Band at 1.98 GHz with 35 dB attenuation level. One spurious frequency appears at 5.9 GHz, approximately three times of first resonance frequency. The layout with dimensions of the designed SB-BSF is shown in Fig. 1. The dimensions are as follows: width of microstrip line $w = 3.1$ mm, the gap $g = 0.35$ mm, $t = 0.53$ mm, $m = 11$ mm, $L = 10.8$ mm, $U = 39.6$ mm and $V = 20$ mm. The simulated frequency response of the SB-BSF is shown in Fig. 2. From the frequency response, it has been observed that it will be useful for frequency 1.98 GHz with 35 dB attenuation level. The spurious frequency also appears at 5.9 GHz with 8 dB attenuation level.

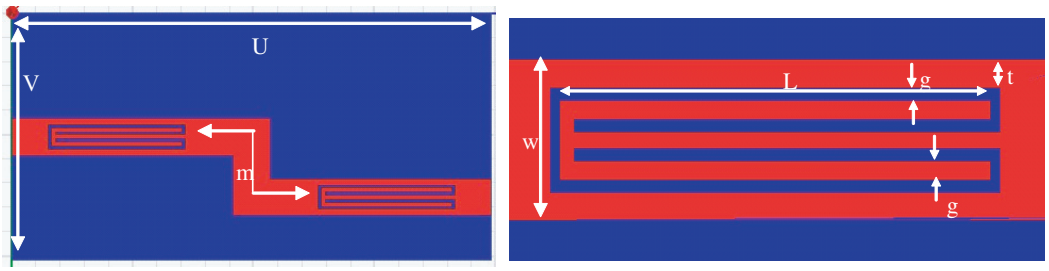

Figure 1. Layout of an SB-BSF). (a) Layout. (b) Dimensions.

The center frequency of the Single-Band to the Quad-Band Bandstop filters can be approximately obtained using expression (1).

$$f_i = \frac{150}{L_i \sqrt{\varepsilon^i_{eff\_s}}} \quad i = 1, 2, 3 \tag{1}$$

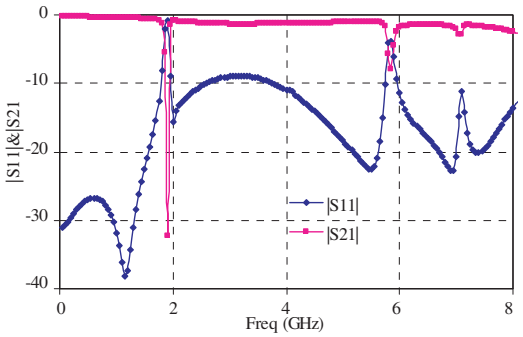

Figure 2. Frequency response of the SB-BSF.

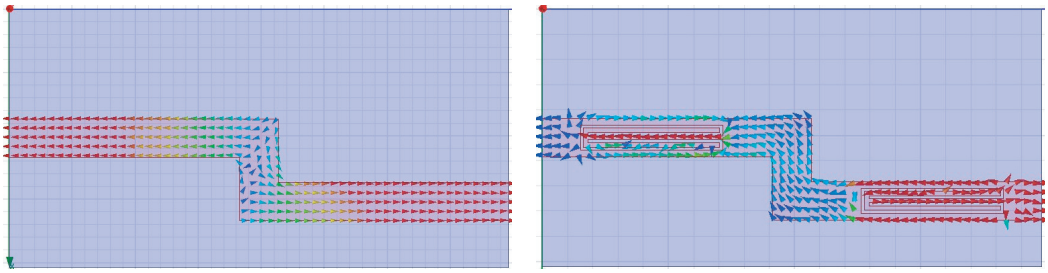

Figure 3. Surface current distribution at 1.9 GHz. (a) In 50 Ω line. (b) In SB-BSF.

where $\varepsilon^1_{eff\_s}$, $\varepsilon^2_{eff\_s}$ and $\varepsilon^3_{eff\_s}$ are the effective dielectric constants for different folded U-slots in microstrip line as well as in the ground plane. L_i is the total length of the folded U-slots. For $0.0015 \leq 0.0083 f_i \leq 0.075$, the effective dielectric constant for the folded U-slots can be obtained using the closed-form expressions [18] given in Equation (2).

$$\frac{1}{\sqrt{\varepsilon^i_{eff\_s}}} = 0.9717 - 0.277 \ln \varepsilon_r + 0.0322 \left(\frac{W_i}{h}\right) \left[\frac{\varepsilon_r}{\left(\frac{W_i}{h} + 0.435\right)}\right]^{1/2} - 0.01 \ln\left(\frac{h f_i}{c}\right) \left[4.6 - \frac{3.65}{\varepsilon_r^2 \sqrt{\frac{W_i f_i}{c}\left(9.06 - \frac{100 W_i c}{f_i}\right)}}\right] \quad (2)$$

The surface current distribution is shown in Fig. 3 for both 50 Ω line and in the SB-BSF at resonance frequency 1.9 GHz. The direction of the stored surface current in the 50 Ω line is outward at both the ends in the microstrip line, while the directions of surface currents in the folded U-slots are in opposite directions, thus the magnetic fields produced by these surface currents will cancel out. These slots store only electric fields, which are responsible for the creation of the Single-Band Bandstop at 1.9 GHz. Similar surface current distributions also appear for the spurious resonance frequency at 5.9 GHz; however, the intensity of the stored currents is small compared with the surface current distribution at 1.9 GHz. Hence the spurious frequency has only 7 dB attenuation level. For all other frequencies, the direction of the stored currents in the SB-BSF are outwards at both the end of the microstrip line.

The fractional bandwidth is calculated by using Equation (3), where $f_{\max}$ and $f_{\min}$ are the 3 dB

frequencies, and f_0 is the central resonance frequency.

$$FBW = \frac{f_{\max} - f_{\min}}{f_0} \tag{3}$$

$$Q_L = \frac{f_0}{f_{\max} - f_{\min}} = \frac{f_0}{3\,\text{dB}\,BW} \tag{4}$$

$$Q_E = \frac{f_0}{FBW} \tag{5}$$

The Loaded quality factor (Q_L) and external quality factor (Q_E) can be obtained using expressions (4) and (5). The fractional bandwidth (% FBW) is 6.52%, the loaded quality factor Q_L 15.32 and the external quality factor Q_E 28.9. However, the return loss (RL) is 0.8 dB. Hence another Single-Band frequency can be stopped by changing the dimensions of the folded U-slots. The proposed SB-BSF can be useful to stopping the interference of GSM frequency with the other frequency band.

2.2. Dual-Band Bandstop Filter (DB-BSF)

The DB-BSF has been designed by adding one more folded U-slot in center of the microstrip line. The dimensions of the folded U-slots can be obtained using Equation (1) for the specified frequency. The addition of extra folded U-slot in the center creates another stop band at 2.9 GHz; however, the first stop band obtained using two slots remains almost at the same frequency 1.9 GHz. Likewise in the SB-BSF, one spurious frequency band also appears in DB-BSF at the same frequency 5.9 GHz with 7 dB attenuation level. Three folded-U slots are used in the microstrip line to stop the two unwanted frequencies simultaneously from the WLAN and UWB band. The layout and dimensions of the DB-BSF are presented in Fig. 4. The dimensions of the outer two folded-U slots are same as that we have taken in SB-BSF; however, the dimensions of the central slot are as follows: width of microstrip line w = 3.1 mm, gap g = 0.35 mm, t = 0.53 mm and L = 6.5 mm. The simulated frequency response of the DB-BSF is shown in Fig. 5. It has two stopband frequencies at 1.9 GHz and 2.9 GHz with attenuation levels 19 dB and 25 dB, respectively. Using this filter, the interference of GSM and 2.9 GHz bands can be stopped from the WLAN bands.

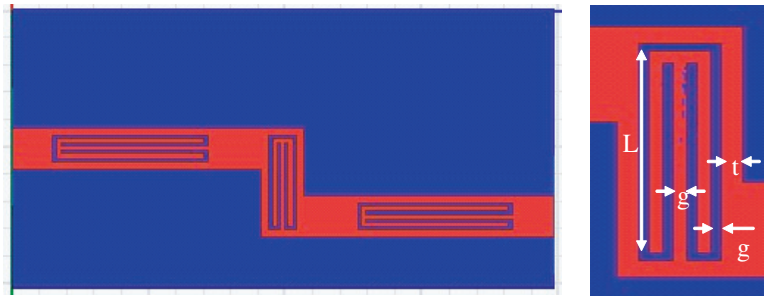

Figure 4. Layout and dimensions of DB-BSF. (a) Layout. (b) Central slot.

The surface currents distributions in DB-BSF are demonstrated in Fig. 6 for both resonance frequencies. At resonance frequency 1.9 GHz, the maximum current is distributed in both the outer slots; however, the current distributed in the central slot is small. The directions of the distributed currents for 1.9 GHz in both the outer slots are in opposite directions, while the direction of distributed current in central slot is in the same direction, hence outer slots are responsible for the first resonance frequency. For 2.9 GHz the directions of distributed surface currents in central slot are in opposite directions; however, the directions of surface currents in the outer slots are in the same direction. Hence the central slot is responsible for creating the second resonance frequency. The magnetic fields produced by this surface current cancel out for frequencies 1.9 GHz and 2.9 GHz. The stored electric fields are responsible for the creation of Dual-Band frequency response. Similar surface current distributions also

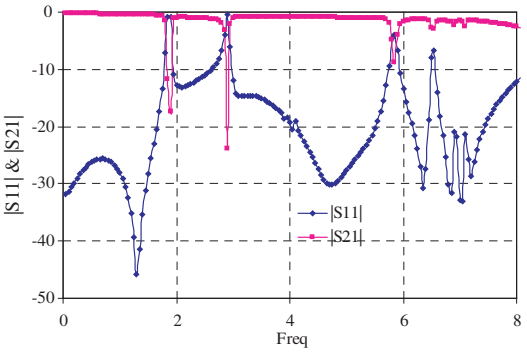

Figure 5. Frequency response of DB-BSF.

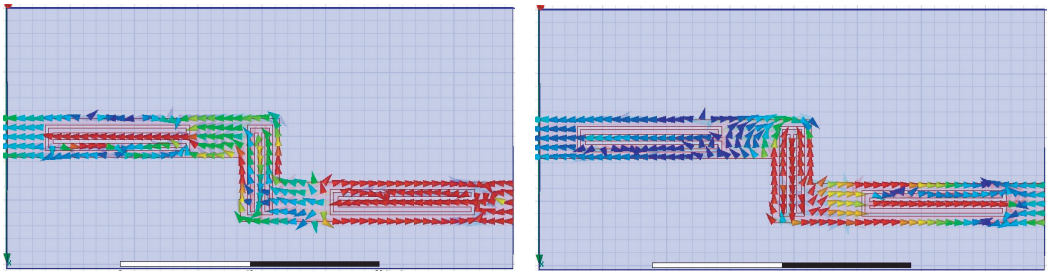

Figure 6. Surface current distribution in DB-BSF. (a) At 1.9 GHz. (b) At 2.9 GHz.

appear for the third spurious resonance frequency at 5.9 GHz; however, the intensity of these stored currents is small compared with the surface current distribution at 1.9 GHz and 2.9 GHz. Hence the spurious frequency has only an attenuation level of 7 dB. On all other frequencies, the directions of the stored currents in DB-BSF are outwards at both ends of the microstrip line. The performances of the DB-BSF are as follows: The fractional bandwidths (% FBW) are 6.8% and 3.5%; the loaded quality factors Q_L are 14.71 and 28.6; the external quality factors Q_E are 28.9 and 82.8; however, the insertion loss (IL) between two stop bands is 0.8 dB. DB-BSF frequencies can be varied by changing the dimensions and controlling the mutual coupling between the slots.

2.3. Triple-Band Bandstop Filter (TB-BSF)

In Single-Band and Dual-Band the folded 50 Ω microstrip line has been used while for the design of a TB-BSF, straight microstrip line has been considered. Again to design the TB-BSF, three folded U-slots in the microstrip line have been used. The sizes of the folded U-slots are obtained using Equation (1). Two outer slots are used to get the first resonance frequency at 2.0 GHz; however, the central slot is used to obtained the second resonance frequency at 4.76 GHz. By changing the slot gap width from 0.35 mm to 0.3 mm, the coupling of electric field between the slots will be enhanced, and the spurious resonance appearing in SB-BSF and DB-BSF becomes the third resonance frequency in the TB-BSF. This TB-BSF is useful for frequencies 2.0 GHz, 4.76 GHz, 6.56 GHz with attenuation levels 32 dB, 30 dB and 22 dB, respectively. The layout and dimensions of the TB-BSF are shown in Fig. 7. The outer two folded-U slots are symmetrical, hence the dimensions of both the slots are the same as follows: width of microstrip line $w = 3.1$ mm, the gap $g = 0.3$ mm, $g_1 = 0.45$ mm, $t = 0.33$ mm, $t_1 = g = 0.3$ mm, $L_1 = 9.7$ mm, $m = 3.8$ mm and $L_2 = 3.7$ mm. The simulated and measured frequency responses of the TB-BSF is presented in Fig. 8. The fabricated TB-BSF is shown in Fig. 11.

The surface current distribution in the microstrip line has been used to understand the working of a TB-BSF. The surface current distributions in the TB-BSF have been demonstrated in Fig. 9 for all the three resonance frequencies. The maximum current for resonance frequency 2.0 GHz is distributed

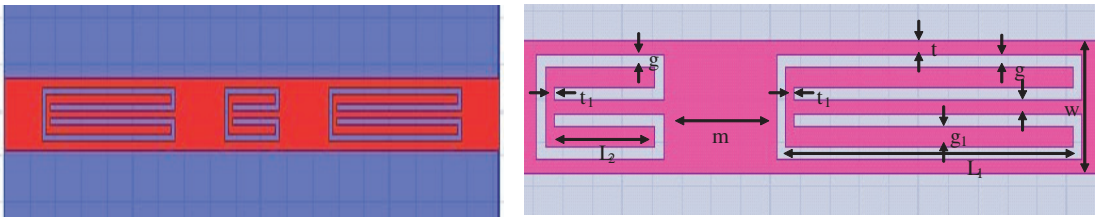

(a) (b)

Figure 7. Layout of the TB-BSF. (a) Layout. (b) Dimensions.

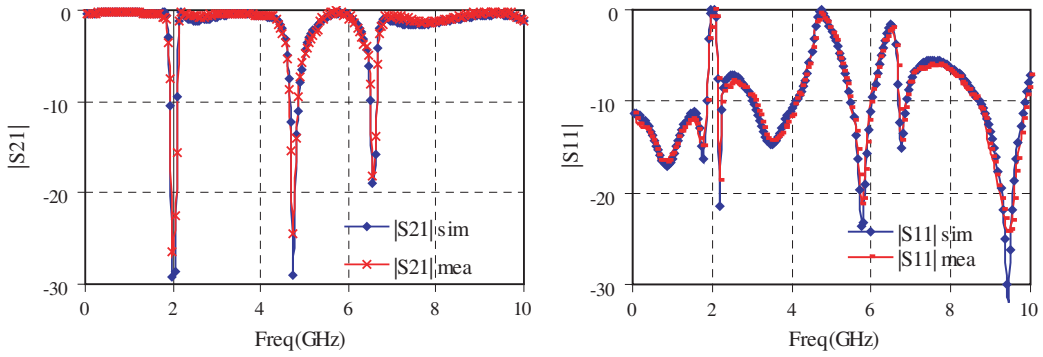

(a) (b)

Figure 8. Frequency response of the TB-BSF. (a) $|S_{21}|$ Response. (b) $|S_{11}|$ Response.

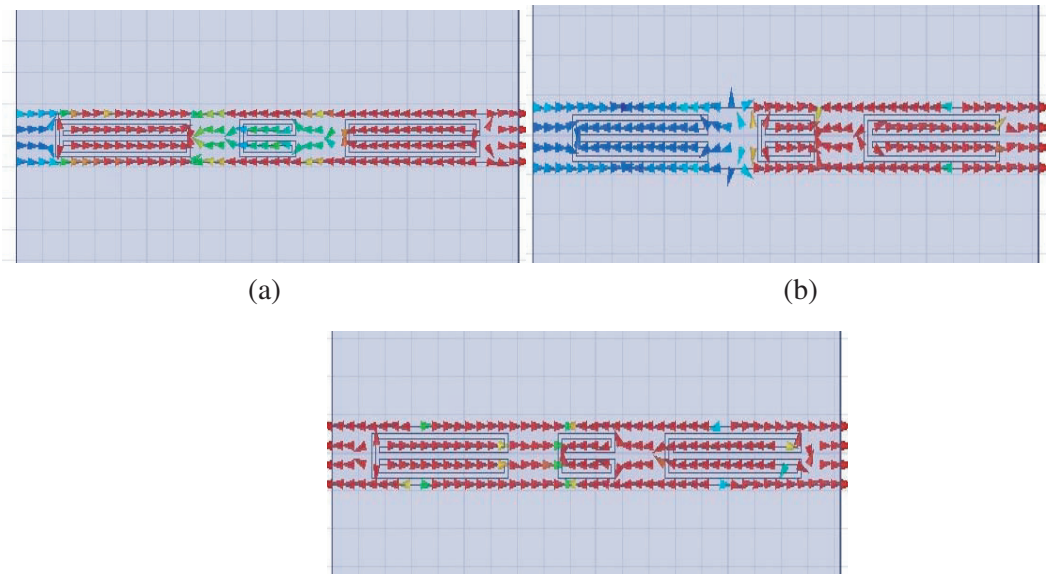

(a) (b)

(c)

Figure 9. Surface current distribution in the TB-BSF. (a) At 2.0 GHz. (b) At 4.76 GHz. (c) At 6.56 GHz.

in both the outer slots; however, the current distributed in the central slot is small. Both outer slots are responsible for the creation of stop band at 2.0 GHz. For 4.76 GHz, the distributed surface currents in central slot and in right-hand side outer slot are maximum. Hence, the central slot and right-hand side outer slot are responsible for the creation of the second resonance frequency. For the third resonance frequency 6.56 GHz, all the three slots have uniform surface current distribution. Hence, the mutual coupling of the fields in these three slots is responsible for the creation of third resonance frequency.

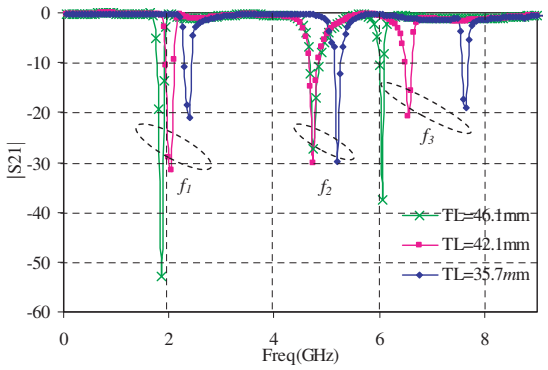

Figure 10. $|S_{21}|$ response with the size (total length) of side folded U-slot.

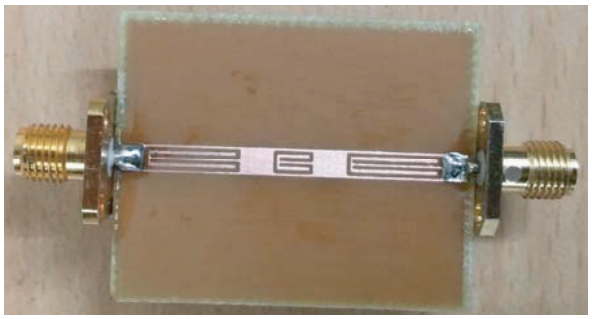

Figure 11. Fabricated TB-BSF.

The fractional bandwidths (% FBW) are 11.5%, 10.5% and 4.4%; the loaded quality factors Q_L are 8.7, 9.5 and 22.7; the external quality factors Q_E are 17.4, 44.6 and 146.2 at 2.0 GHz, 4.76 GHz, 6.56 GHz frequencies; however, the insertion loss (IL) between these three stop bands are 0.31 dB, 0.9 dB and 0.32 dB. To investigate the effect of size (total length) of the folded U slot on the stop band frequencies f_1, f_2 and f_3, the outer side slots have been considered, and their sizes (total lengths) are changed from 46.1 mm to 42.1 mm and to 35.7 mm. The frequencies f_1, f_2 and f_3 are changed from 1.85 GHz, 4.75 GHz, and 6.05 GHz to 2.0 GHz, 4.76 GHz, and 6.56 GHz and to 2.4 GHz, 5.2 GHz and 7.65 GHz, which can be clearly seen in Fig. 10. To further investigate the mutual coupling between the central slot and the side slots, the TB-BSF with different relative positions (m) of the side slots with the central slot are examined. The frequencies f_1, f_2 and f_3 are changed from 2.0 GHz, 4.76 GHz, and 6.56 GHz to 2.1 GHz, 4.76 GHz, and 6.67 GHz to 2.15 GHz, 4.76 GHz, and 6.70 GHz by changing m from 3.8 mm to 2.8 mm and 1.8 mm. It has been observed that the central frequency (f_2) keeps almost the same when m changes.

Hence, the frequencies of the TB-BSF can be varied by changing the dimensions and controlling the mutual coupling between the slots. Table 1 compares the performances of our proposed TB-BSF with the previously reported TB-BSF. Our proposed TB- BSF has smaller size than the filters reported in [7, 8] and [10–13].

Table 1. Performance of triple band BSF.

Ref	Frequency (GHz)			F.B.W (%)			Loaded Q_L			Substrate parameters		
	f_1	f_2	f_3	f_1	f_2	f_3	f_1	f_2	f_3	ε_r	h (mm)	Size (mm^2)
[7]	0.9	1.59	2.15	15.55	14.01	11.42	6.43	7.14	8.75	4.6	0.8	15.2 × 82.4
[8]	2.16	3.98	5.96	8.79	23.4	14.1	11.37	4.28	7.10	10.2	1.27	32 × 12
[9]	2.04	2.87	3.97	12.5	11.8	13.9	7.85	8.44	7.22			10 × 5
[10]	2.5	3.2	4.7	5.2	12.2	11.3	19.2	8.2	8.8	10.2	1.27	25.6 × 16
[11]	2.37	3.54	5.01	6.33	3.95	3.79	15.8	25.3	26.4	2.55	1.5	41.6 × 8.4
[12]	2.56	3.42	4.08	12.1	2.93	2.45	8.26	34.2	40.2	10.2	1.27	31.2 × 16.2
[13]	2.36	3.48	5.16	6.36	9.19	8.67	15.73	10.87	11.53	2.2	1.575	21.1 × 9.1
[14]	2.59	6.38	10.67	46.28	16.22	8.05	2.13	5.21	11.48	2.52	0.504	20 × 6.4
Our (sim)	**2.0**	**4.76**	**6.56**	**11.5**	**10.5**	**4.4**	**8.7**	**9.5**	**22.7**	**4.4**	**1.6**	**39.6 × 4.5**
Our (mea)	**2.1**	**4.86**	**6.66**	**11.6**	**11.0**	**4.5**	**8.5**	**10.0**	**23.7**	**4.4**	**1.6**	

3. DESIGN OF QUAD-BAND TO HEXA-BAND BANDSTOP FILTER

This section presents the design of the Quad-Band (QB-BSF) to the Hexa-Band (HB-BSF) Bandstop filters by using the microstrip line with embedded folded U-slots as well as embedded U-slots in the ground plane and also one coupled S-type resonator. These three filters are useful to stopping the unwanted signal frequency from 2.0 GHz to 7.75 GHz in WLAN and UWB band.

3.1. Quad-Band Bandstop Filter (QB-BSF)

To design the QB-BSF, Equations (1) and (2) are used to find the dimensions of the folded U-slots. Both microstrip line and ground plane are used to design the QB-BSF. However, article [15] reported a QB-BSF using defected microstrip structure (DMS) and E-shaped defected ground structure (DGS) with open-loop resonators coupled to the microstrip line. Article [16] reported using two shunt-connected tri-section stepped-impedance resonators (TSSIRs) and article [17] using open-circuited stubs. Above reported articles have good Quad-Band Bandstop frequency response though they have complex structures and difficulty to control the frequency bands. Layout and dimensions of the proposed QB-BSF are shown in Fig. 12. The top side structure of the proposed QB-BSF has the same dimensions as that of the TB-BSF, shown in Fig. 7(b). The dimensions of the ground plane structure are as follows: $L_2 = 6.3\,\text{mm}$, $g_2 = 0.3\,\text{mm}$, $g_3 = 0.6\,\text{mm}$, $m_2 = 7.2\,\text{mm}$. The simulated and measured frequency responses are presented in Fig. 13. The proposed QB-BSF is useful for frequencies 2.0 GHz, 3.3 GHz, 4.75 GHz and 6.5 GH. The surface current distributions in the microstrip line as well as in the ground

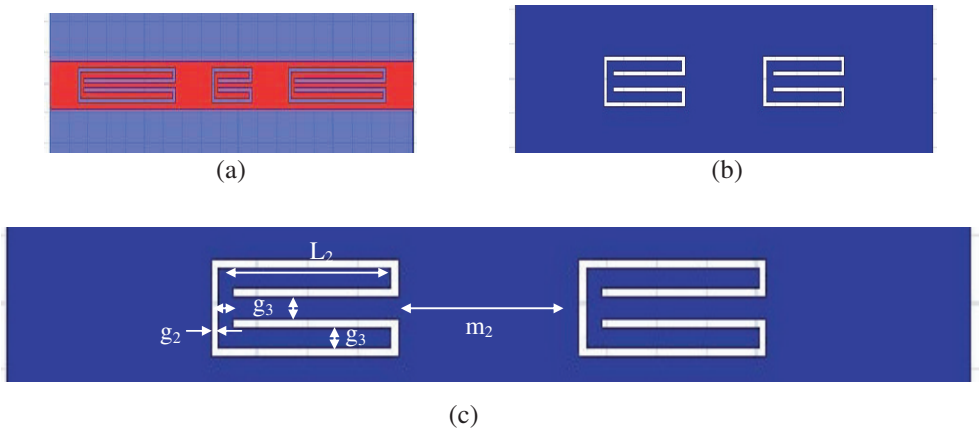

Figure 12. Layout of the QB-BSF. (a) Top side. (b) Bottom side. (c) Dimension of bottom side.

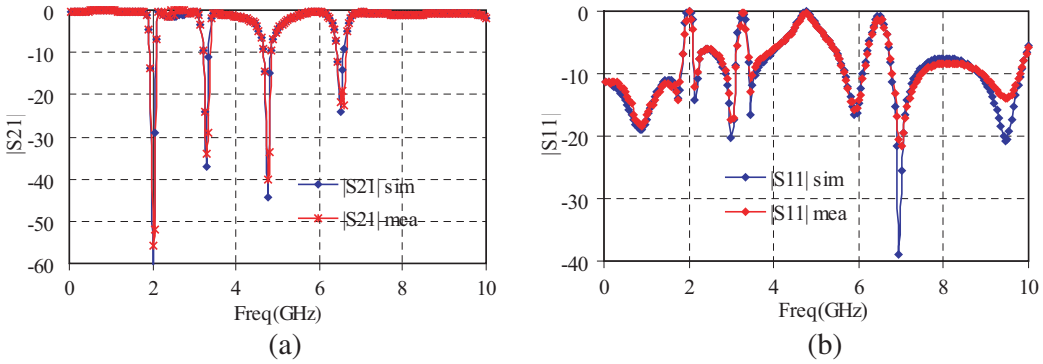

Figure 13. Simulated and Measured frequency response of the QB-BSF. (a) $|S_{21}|$ Response. (b) $|S_{11}|$ Response.

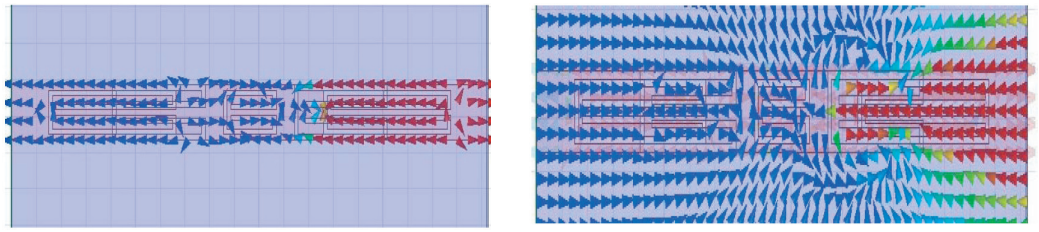

(a) (b)

Figure 14. Surface current distribution in the QB-BSF at 2.0 GHz. (a) Top side. (b) Bottom side.

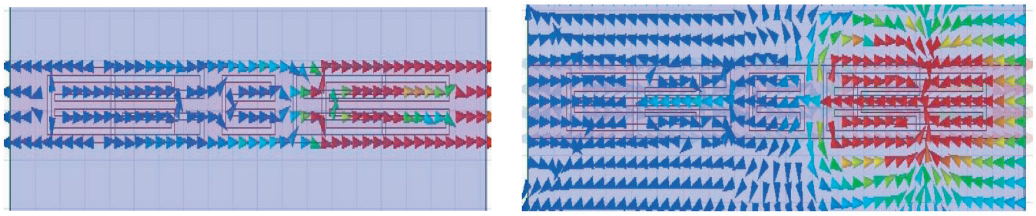

(a) (b)

Figure 15. Surface current distribution in the QB-BSF at 3.3 GHz. (a) Top side. (b) Bottom side.

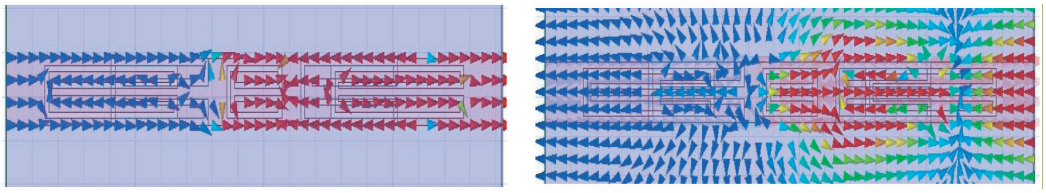

(a) (b)

Figure 16. Surface current distribution in the QB-BSF at 4.76 GHz. (a) Top side. (b) Bottom side.

plane have been presented to understand the working of the QB-BSF. The surface current distributions in the QB-BSF have been demonstrated in Fig. 14 to Fig. 17 for all the four resonance frequencies.

The maximum current is distributed in the right-hand side of the outer slot for resonance frequency 2.0 GHz as shown in Fig. 14. In ground plane, the current makes loop, hence right-hand side slot in microstrip line is responsible for the first resonance frequency at 2.0 GHz. For the second resonance frequency 3.3 GHz, the current is mainly distributed in right-hand side slots in both microstrip line and ground plane shown in Fig. 15, hence the right-hand side slot in ground plane is responsible for the creation of the second resonance frequency. For the third resonance frequency at 4.76 GHz, the maximum currents are distributed in central slot and right-hand side slot shown in Fig. 15. The right-hand side slot and central slot in microstrip line are responsible for the third resonance frequency.

For the fourth resonance frequency, the distributed currents in all the three slots in microstrip line and in the left-hand side slot in ground plane are shown in Fig. 17. Hence, left-hand side slot in the ground plane and all the three slots in the microstrip line are responsible for the fourth resonance at 6.5 GHz. The fractional bandwidths (% FBW) are 10.8%, 7.4%, 12.5% and 5.5%; the loaded quality factors Q_L are 9.2, 13.5, 7.9 and 18.1; the external quality factors Q_E are 18.3, 44.7, 37.8 and 153.5 at resonance frequencies 2.0 GHz, 3.3 GHz, 4.75 GHz and 6.5 GHz, respectively. The insertion losses (IL) between the four stop bands are 0.31 dB, 1.2 dB, 1.2 dB and 0.38, respectively. Like TB-BSF, the frequencies of the QB-BSF can be varied by changing the dimensions and controlling the mutual coupling between the slots. The simulated and measured frequency responses of the QB-BSF are presented in Fig. 13. Fabricated QB-BSF is shown in Fig. 18. Table 2 compares the performances of our proposed

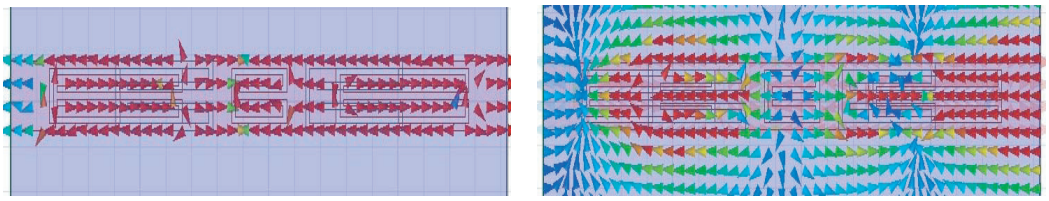

(a) (b)

Figure 17. Surface current distribution in QB-BSF at 6.5 GHz. (a) Top side (b) Bottom side.

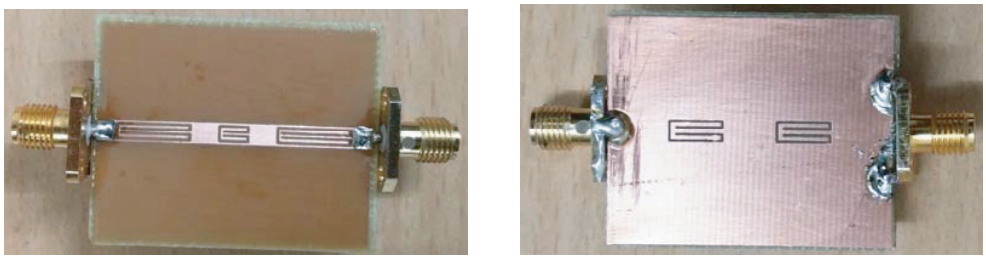

(a) (b)

Figure 18. Fabricated QB-BSF. (a) Top side. (b) Bottom side.

Table 2. Performance of QB-BSF.

Ref.	Frequency (GHz)				F.B.W (%)				Loaded Q_L			
	f_1	f_2	f_3	f_4	f_1	f_2	f_3	f_4	f_1	f_2	f_3	f_4
[15]	2.37	3.52	5.20	5.70	7.8	5.7	4.60	4.9	12.8	17.5	21.7	20.4
[16]	1.74	3.56	5.67	8.52	61.8	44.9	35.80	8.04	1.63	2.20	2.80	12.26
Our (sim)	**2.0**	**3.30**	**4.75**	**6.45**	**21.8**	**24.5**	**59.6**	**35.5**	**9.2**	**13.5**	**7.9**	**18.1**
Our (mea)	**2.1**	**3.35**	**4.84**	**6.50**	**21.7**	**24.2**	**60.1**	**34.8**	**9.3**	**13.6**	**7.6**	**18.8**

Ref	External Q_{EXT}				Attenuation (dB)				Substrate parameters and Size		
	f_1	f_2	f_3	f_4	f_1	f_2	f_3	f_4	ε_r	h (mm)	Size (mm^2)
[15]	30.4	61.8	113.0	117.6	36.7	32.3	31.4	25.0	2.55	1.5	39.9 × 22.15
[16]	2.82	7.93	15.84	106.7	31.2	39.0	18.2	20.0	10.2	1.27	10 × 10
Our (sim)	**18.4**	**44.7**	**37.9**	**115.5**	**33.6**	**43.3**	**22.7**	**28.7**	**4.4**	**1.6**	**39.6 × 4.5**
Our (mea)	**18.9**	**45.1**	**37.2**	**116.2**	**32.1**	**41.5**	**20.1**	**24.5**	**4.4**	**1.6**	**39.6 × 4.5**

QB-BSF with the previously reported QB-BSFs. Our proposed QB-BSF has a smaller size than the filters reported in [15]. The size of [16] has a smaller size than our proposed filter; however, the loaded quality factors are smaller, and also the controls of resonance frequencies are difficult.

3.2. Penta-Band (PB-BSF) and Hexa-Band Bandstop Filter (HB-BSF)

Till now, the microwave community is able to design bandstop filters up to the Quad-Band [15–17], the Penta-Band and Hexa-Band bandstop filters are difficult to design, hence no such bandstop filters are available in the open literature. This section deals with design of the PB-BSF and HB-BSF. To design

the PB-BSF and HB-BSF, folded U-slots are used in both microstrip line and ground plane with one S-type coupled resonator to microstrip line. For the specified frequencies, the dimensions of the folded U-slots are obtained using Equations (1) and (2). The five resonance frequencies f_1, f_2, f_3, f_4 and f_5 can be rejected simultaneously by using the PB-BSF. The first (f_1), second (f_2), fourth (f_4) and fifth (f_5) resonance frequency bands can be created using folded U-slots both in microstrip line and ground plane; however, the third resonance frequency can be created by placing an S-type resonator near the microstrip line.

For frequencies f_1, f_2, f_4 and f_5, Equations (1) and (2) are used to obtain the dimensions of the slots; however, for frequency f_3, the dimension of the S-type resonator (half-wavelength resonator) is obtained using Equations (6) and (7).

$$f_i = \frac{150}{d\sqrt{\varepsilon_{eff}}} \tag{6}$$

$$\varepsilon_{eff} = \frac{\varepsilon_r + 1}{2} + \frac{\varepsilon_r - 1}{2} \frac{1}{\sqrt{1 + 12h/W}} \tag{7}$$

where $d = 3L_3 + 2L_4 + 3g_4$ and $W = g_4$ are total length and width of the coupled S-type resonator. The layout and dimensions of the PB-BSF are shown in Fig. 19. The dimensions of the top side and ground plane are the same as we have considered for the TB-BSF and the QB-BSF, shown in Fig. 7(b) and Fig. 12(c). The dimensions of the coupled S-type resonator (half-wavelength resonator) are as follows: $L_3 = 5.9\,\text{mm}$, $L_4 = 2.2\,\text{mm}$, $g_4 = 0.5\,\text{mm}$ and $g_5 = 0.25\,\text{mm}$, shown in Fig. 19(c). The simulated and measured frequency responses of the PB-BSF are presented in Fig. 20. This PB-BSF is useful for frequencies 2.0 GHz, 3.4 GHz, 4.0 GHz, 4.85 GHz and 6.75 GHz with 38 dB, 35 dB, 23 dB, 47 dB and 20 dB attenuation levels, respectively. The performances of the PB-BSF are as follows: fractional bandwidths (% FBW) are 10.3%, 7.4%, 5.3%, 12.9% and 5.6%; the loaded quality factors Q_L are 9.7, 13.6,18.9, 7.7 and 17.6; the external quality factors Q_E are 19.8, 44.7, 73.7, 36.7 and 111.7 at resonance frequencies 2.0 GHz, 3.4 GHz, 4.0 GHz, 4.85 GHz and 6.75 GHz respectively. The insertion losses (IL)

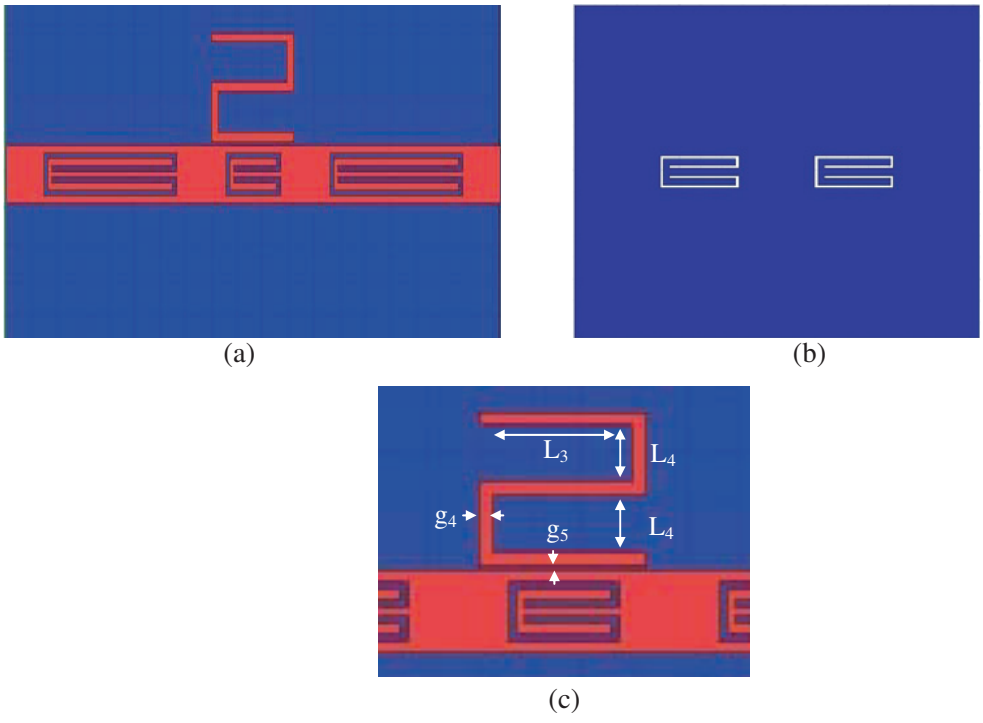

Figure 19. Layout of the PB-BSF and HB-BSF. (a) Top side. (b) Bottom side. (c) Dimensions of S-type resonator.

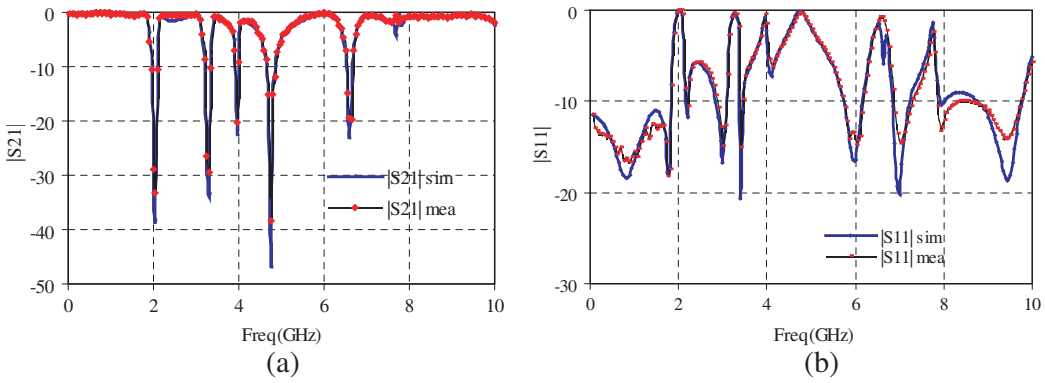

Figure 20. Simulated and measured frequency responses of the PB-BSF. (a) $|S_{21}|$ response. (b) $|S_{11}|$ Response.

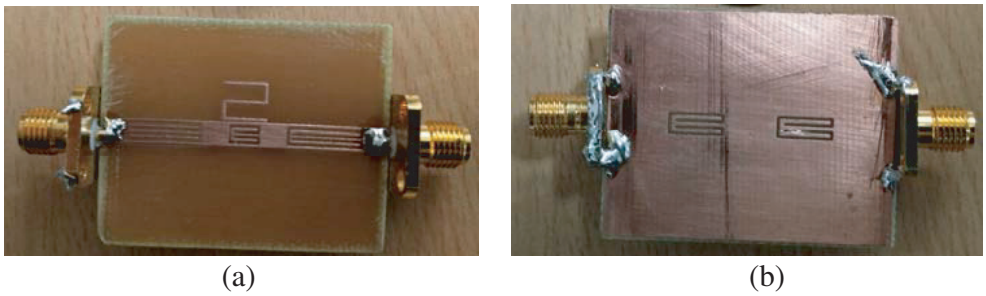

Figure 21. Fabricated PB-BSF and HB-BSF. (a) Top side. (b) Bottom side

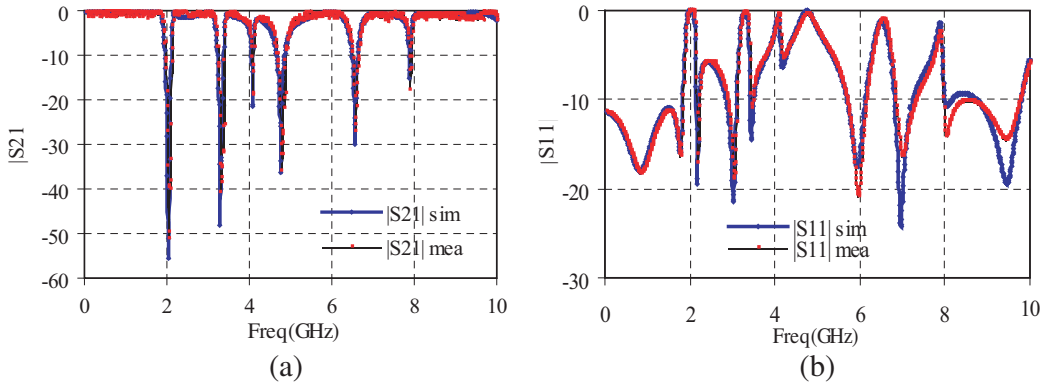

Figure 22. Simulated and Measured frequency response of the PB-BSF.

among the five stop bands are 0.31 dB, 1.2 dB and 1.2 dB, 0.9 dB and 0.38 dB, respectively. By changing the size of the S-type resonator from $L_3 = 5.9$ mm, $L_4 = 2.2$ mm, $g_4 = 0.5$ mm and $g_5 = 0.25$ mm to $L_3 = 5.9$ mm, $L_4 = 1.95$ mm, $g_4 = 0.5$ mm and $g_5 = 0.25$ mm, the Hexa-Band operation can be obtained. The PB-BSF and HB-BSF have actually the same circuit. It can be observed from Fig. 20 and Fig. 22 that the sixth stop band is actually the spurious frequency of the third stop band frequency (nearly two times, namely the first spurious frequency of the half-wavelength resonator) in the responses of the Penta-Band. By changing the length of the half-wavelength resonator, the sixth stop band is matched and formed. Therefore, both the filters are discussed together in the same section.

The fabricated PB-BSF and HB-BSF are similar and the difference only in the dimensions of the coupled S-type resonator (half-wavelength resonator) shown in Fig. 21. The simulated and measured

frequency responses of the HB-BSF is shown in Fig. 22. The HB-BSF can be useful for frequencies 2.0 GHz, 3.34 GHz, 4.0 GHz, 4.74 GHz, 6.43 GHz and 7.8 GHz with attenuation levels 51.8 dB, 45.3 dB, 29.4 dB, 37.1 dB and 15.1 dB, respectively.

The surface current distributions for different frequencies have also been used to understand the working mechanism of both the PB- and HB-BSFs. To save the space, the surface current distribution in the PB- and HB-BSFs at different frequencies are not presented here. The fractional bandwidths (% FBW) are 9.5%, 6.9%, 4.4%, 12.3%, 4.3%, and 2.1%, the loaded quality factors Q_L are 10.5, 14.4, 22.7, 8.2, 23.4, and 49.3; the external quality factors Q_E are 21.7, 48.1, 91.5, 38.7, 150.3, and 384.5 at resonance frequencies 2.05 GHz, 3.34 GHz, 4.10 GHz, 4.76 GHz, 6.57 GHz and 7.92 GHz respectively. The insertion losses (IL) among the six stop bands are 0.31 dB, 1.2 dB, 1.5 dB, 2.1 dB, 0.5 dB and 0.38 respectively. HB-BSF frequencies can be varied by changing the dimensions and controlling the mutual coupling between the slots and S-type resonator. The simulated and measured frequency responses of the HB-BSF is presented in Fig. 22. Fabricated HB-BSF is shown in Fig. 21.

4. CONCLUSION

A systematic design methodology has been presented to design the Multi-Band Bandstop filters from the Single-Band BSF (SB-BSF) to the Hexa-Band BSF (HB-BSF). The presented BSFs are useful to suppress the unwanted signal frequencies from 1.98 GHz to 7.75 GHz. The attenuation level for suppressed frequencies varies from 19 dB to 62 dB, and the quality factor varies from 17 to 384.5. The surface current distributions have been used to understand the working mechanism of the filters. Finally, some of the Bandstop filters are fabricated, and their measured results are presented to validate the design process. Such compact BSFs could be used in modern communication systems to stop the potential interference of the unwanted signal frequencies in WLAN and UWB band.

ACKNOWLEDGMENT

This work was supported by Delhi University Innovation Project 2015-2016.

REFERENCES

1. La, D.-S., W.-H. Han, and J.-L. Zhang, "Compact band-stop filters using π-Shape DGS and π-shape DMS," *Microwave and Optical Technology Letters*, Vol. 56, No. 11, 2504–2507, November 2014.
2. Wang, J., H. Ning, L. Mao, and M. Li, "Miniaturized dual-band bandstop filter using defected microstrip structure and defected ground structure," *2012 IEEE MTT-S International Microwave Symposium Digest (MTT)*, 1–3, Montreal, QC, Canada, 2012.
3. Uchinda, H., H. Kamino, K. Totani, N. Yoneda, M. Miyazaki, Y. Konishi, S. Makino, J. Hirokawa, and M. Ando, "Dual-band-rejection filter for distortion reduction in RF transmitters," *IEEE Trans. Mirow. Theory Tech.*, Vol. 52, No. 11, 2550–2556, November 2004.
4. Chin, K. S., J. H. Yeh, and S. H. Chao, "Compact dual-band bandstop filters using stepped-impedance resonators," *IEEE Microw. Wireless Component Lett.*, Vol. 17, No. 12, 849–851, December 2007.
5. Chiou, H. K. and C. F. Tai, "Dual-band microstrip bandstop filter using dual-mode loop resonator," *Electronic Lett.*, Vol. 45, No. 10, 507–509, May 2009.
6. Verma, A. K., A. Abdel-Rahman, A. Kumar, A. Balalem, and A. Omar, "New compact dual-band bandstop filter," *International Journal of Electronics, Taylor & Francis*, Vol. 100, No. 4, 497–507, 2013.
7. Liao, S.-S., S.-Y. Yuan, Y.-L. Wu, and T.-Y. Huang, "Compact microstrip bandstop filter with controllable triple stopband response," *PIRS Proceedings*, 1377–1380, Kula Lumper, Malaysia, March 27–30, 2012.

8. Xiao, J.-K. and Y.-F. Zhu, "Multiband bandstop filter using inner T-shaped defected microstrip structure (DMS)," *International Journal of Electronics and Communication (AEU)*, Vol. 68, 90–96, 2014.
9. Chiu, L. and Q. Xue, "A simple microstrip bandstop filter using cross-coupling stubs," *International Journal of Microwave Science and Technology*, Article ID 473030, 2012.
10. Xiao, J. K. and H. F. Huang, "Square patch resonator banstop filter," *12th IEEE International Conference on Communication Technology (ICCT)*, 104–107, November 11–14, 2010.
11. Ning, H., J. Wang, Q. Xiong, and L.-F. Mao, "Design of planar dual and triple narrow-band bandstop filters with independently controlled stopbands and improved spurious response," *Progress In Electromagnetics Research*, Vol. 131, 259–274, 2012.
12. Xiao, J.-K. and Y.-F. Zhu, "New U-shaped DGS bandstop filters," *Progress In Electromagnetics Research C*, Vol. 25, 179–191, 2013.
13. Jankovic, N., R. Geschke, and V. C. Bengin, "Compact tri-bnad bandpass and bandstop filters based on Hilbert-Fork resonators," *IEEE Microwave and Wireless Components Letters*, Vol. 23, No. 6, June 2013.
14. Dhakal, R. and N. Y. Kim, "A compact systematic microstrip filter based on a rectangular meandered line stepped impedance resonator with a triple band bandstop response," *The Scientific World Journal*, Vol. 2013, article ID 457693, 2013.
15. Ning, H., J. Wang, Q. Xiong, H. Liu, and L. Mao, "A compact quad-band bandstop filter using dual-plane defected structures and open-loop resonators," *IEICE Electronics Express*, Vol. 9, No. 21, 1630–1636, 2012.
16. Adhikari, K. K. and N. Y. Kim, "A miniaturized quad-band bandstop filter with high selectivity based on shunt-connected, T-shaped stub-loaded, stepped-impedance resonators," *Microwave and Optical Technology Letters*, Vol. 57, No. 5, 1129–1132, May 2015.
17. Karpuz, C., A. Gorur, A. K. Gorur, and A. Ozek, "A novel compact quad-band microstrip bandstop filter design using open-circuited stubs," *IEEE MTT-S International Microwave Symposium Digest (IMS)*, 1–3, Seattle, WA, 2013.
18. Gupta, K. C., R. Garg, I. Bahl, and P. Bhartia, *Microstrip Lines and Slotlines*, 2nd Edition, Artech House, Norwood, 1996.
19. FCC DA 13-1193, May 2013.
20. Ansoft HFSS ver. 11.